Asian Journal of Chemistry; Vol. 25, No. 12 (2013), 6635-6638

ASIAN JOURNAL OF CHEMISTRY

http://dx.doi.org/10.14233/ajchem.2013.14394

Synthesis and Characterization of Al-TiO_2/ZnO and Fe-TiO_2/ZnO Photocatalyst and Their Photocatalytic Behaviour

SHAHRAM MORADI[1], PARVIZ ABEROOMAND-AZAR[2], SANAZ RAEIS-FARSHID[1,3,*], SAEED ABEDINI-KHORRAMI[1] and MOHAMMAD HADI GIVIANRAD[2]

[1]Department of Chemistry, Tehran North Branch, Islamic Azad University, Tehran, Iran
[2]Department of Chemistry, Science and Research Branch, Islamic Azad University, Tehran, Iran
[3]Department of Chemistry, Lahijan Branch, Islamic Azad University, Lahijan, Iran

*Corresponding author: Fax: +98 21 22222512; Tel: +98 21 22262561; E-mail: s_r_farshid@yahoo.com

(*Received*: 3 August 2012; *Accepted*: 27 May 2013) AJC-13537

The TiO_2/ZnO, Al-TiO_2/ZnO and Fe-TiO_2/ZnO nanocomposites as photocatalysts were prepared by the sol-gel method. The structures and properties were recognized with fourier transform infrared spectroscopy, scanning electron microscopy and X-ray diffraction methods. The XRD studies showed that addition of aluminum and iron to TiO_2/ZnO affected on the particle size of nanocomposite. UV-visible spectrophotometry was used to determine dye concentration. The photocatalytic activity of the synthesized nanocomposites was investigated for decolorization of methyl orange and methylene blue in water under UV irradiation in a batch reactor. The results revealed that the photocatalytic activity of the nanocomposites for decolorization of methylene blue was better than methyl orange.

Key Words: Sol-Gel, Decolorization, Nanocomposite, Methyl orange, Methylene blue.

INTRODUCTION

During recent decades, advanced oxidation processes (AOPs) are a common technique in wastewater purification which can effectively handle various hazardous organics in wastewater[1]. Organic compounds, especially dyes, one of the most important pollutants are in the textile industry. Small amount of these substances creates environmental problems. In recent years with increasing production and use of synthetic dyes that are more complex structure than the natural dye and chemically very stable, it has been paid more attention to environmental pollution[2-4].

Heterogeneous photocatalysis is used for the mineralization of toxic organic pollutants in the environment. Photocatalytic process in polluted water through the use of UV-irradiated inorganic oxides degrades the contaminants[5,6]. Titanium dioxide (TiO_2) as a photocatalyst is used in water purification. Many organic contaminants can be decomposed and mineralized by the proceeding oxidation and reduction processes on TiO_2[4,7]. For improving the photocatalytic activity of TiO_2, different ideas have been investigated. Doping of metal ions has been used to enhance the photocatalytic activity of TiO_2[1,8]. The dopants act as charge separators of photoinduced electron-hole pairs. It is proposed that, after excitation, the electron migrates to the metal where it is trapped and electron-hole recombination is suppressed[9-11]. The coupling of different semiconductors is useful in order to achieve a more efficient electron-hole pair separation under irradiation and a higher photocatalytic activity[12].

Zinc oxide has been conceived as a remarkable candidate that is reportedly known to be more efficient than TiO_2 to degrade organic compounds. The band gap energy of ZnO and TiO_2 is similar to each other (*ca.* 3.2 eV)[13,14].

The sol-gel technique is one of the most suitable technologies for the preparation of nanocomposite. It is suitable to produce nanoparticles and coatings. The advantages of this method are high purity, good uniformity, low temperature synthesis and easily controlled reaction conditions[13-15].

In this work, TiO_2/ZnO, Al-TiO_2/ZnO and Fe-TiO_2/ZnO nanocomposites were prepared by sol gel method. The prepared nanocomposites were characterized by fourier transform infrared spectroscopy (FTIR), scanning electron microscopy (SEM) and X-ray diffraction (XRD) methods. The photocatalytic activity of the synthesized nanocomposites was investigated for decolorization of methyl orange (MO) and methylene blue (MB) in water under UV irradiation in a batch reactor.

EXPERIMENTAL

Tetra isopropyl orthotitanate (TTIP), zinc nitrate tetra hydrate, aluminum nitrate nona hydrate, iron nitrate nona

hydrate, diethanolamine (DEA), glacial acetic acid, methylene blue (MB) and methyl orange (MO) were obtained from Merck. The chemical structure of methylene blue and methyl orange was shown in Fig. 1. Hydroxylpropyl cellulose (HPC) was received from Sigma-Aldrich.

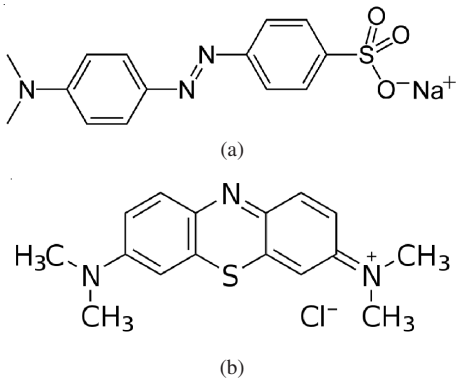

Fig. 1. The chemical structure of (a) methyl orange ($C_{14}H_{14}N_3O_3SNa$) and (b) methylene blue ($C_{16}H_{18}N_3SCl$)

Preparation of nanocomposites: In this study TiO_2/ZnO, Al-TiO_2/ZnO and Fe-TiO_2/ZnO nanocomposites were prepared by sol gel method. The TiO_2 sol was made at room temperature and TTIP was used as a precursor as follows: In the first stage, additive (HPC= 30 g/L) was dissolved in ethanol under fast stirring for 5 min. Then TTIP was dissolved in ethanol with a 1:9 molar ratio of TTIP:ethanol and stirred for 15 min, to obtain a precursor solution. After that, a mixture of absolute ethanol, acetic acid and deionized water with the molar ratio of 10:6:1 was added slowly into the precursor by a fast stirring and it was continuously stirred for 15 min to achieve a yellow transparent sol. Acetic acid was used as an inhibitor to reduce quick hydrolysis of TTIP and to adjust the pH of solution at pH = 5.

Al-ZnO sol was prepared as follows. Firstly zinc nitrate tetra hydrate and aluminum nitrate nona hydrate, were dissolved in absolute ethanol with molar ratios, 0:1, 0.25: 0.75, respectively. After that, stirred for 5 min, then a mixture of absolute ethanol, diethanolamine and deionized water with the molar ratio of 10:2:1 was added slowly into the precursor by a fast stirring and it was continuously stirred for 15 min to achieve transparent sol.

The prepared Al-ZnO sol was added into the TiO_2 acidic sol to get Al-TiO_2/ZnO sol. This sol aged for 24 h. After that, the prepared sol was dried in the air and heat treated at 350 ºC for 10 min then at 500 ºC for 5 h. The samples were naturally cooled after the heat treatment[10,13,15].

The synthesis method of Fe-TiO_2/ZnO nanocomposite was similar to the synthesis method which described above with this difference that iron nitrate nona hydrate was used instead of aluminum nitrate nona hydrate.

Characterization of nanocomposites: FTIR spectra were recorded at room temperature using Thermo Nicolet Nexus 870 FTIR spectrometer. A STADI P, STOE X-ray diffractometer with CuK_α radiation (λ = 0.154060 nm, 40 kV, 30 mA) was used to determine the crystallinity and phase purity of the samples. The XRD pattern were recorded in the 2θ range of 0-100º. Scanning electron microscopy SEM studies were performed with a Hitachi S-4160 Japan.

Evaluation of photocatalytic activity: Experiments were carried out in a batch mode immersion rectangular photocatalytic reactor made of pyrex glass. The radiation source was a UV-C lamp (200-280 nm, 15 W Osram). The schematic representation of the reactor was shown in Fig. 2.

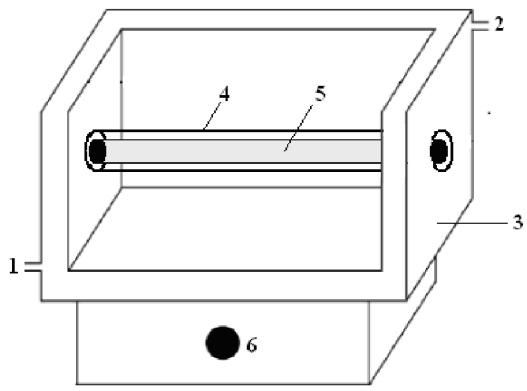

Fig. 2. Schematic diagram of the photoreactor systems. 1.Water input, 2. Water output, 3. Glass jacket, 4. Quartz cover, 5. UV lamp, 6. Stirrer

Photocatalytic decolorization processes were performed using a 1 L solution containing specified concentration of dye. The initial concentration of dye was 5 mg/L. Samples were withdrawn from sample point at certain time intervals and analyzed for decolorization. Decolorization of dye solution was checked and controlled by measuring the absorbance at maximum wavelength (λ_{max} methyl orange) of dye (465 nm) and (λ_{max} methylene blue) of dye (664 nm) at different time intervals by Varian UV-visible spectrophotometer.

RESULTS AND DISCUSSION

FTIR spectra: FTIR spectra of the TiO_2/ZnO, Al-TiO_2/ZnO and Fe-TiO_2/ZnO were shown in Fig. 3, in the wave number range from 4000-400 cm^{-1}. The peaks at 550 and 700 cm^{-1} can be assigned to symmetric stretching vibration of the Ti-O-Ti bond and O-Ti-O, respectively. The peak at 800 cm^{-1} was attributed to the vibration mode of Zn-O-Ti. The peak at 400 and 1400 cm^{-1} was attributed to the vibration mode of Ti-O bond and all those at 1240, 1160 and 1080 cm^{-1} should be due to the Ti-OH bond. The peak at 1650 cm^{-1} resulted from the adsorb H_2O molecules, which were not removed completely after sol-gel synthesis[16-19]. The peaks at 571, 1401 and 1640 cm^{-1} assigned to Fe-O-Ti bond. The peak at 542 cm^{-1} are mainly associated with vibration of Fe-O group[20,21]. The peak at 800-500 cm^{-1} was attributed to Al-O stretching mode and the peaks at 1232, 1460, 1482 and 1620 cm^{-1} should be due to Al-O-Ti bond[22,23]. The wide peak at 3250 cm^{-1} has been assigned to the OH stretching vibration of surface hydroxyl group. During the hydrolysis of TTIP, large amount of ethanol lead to the appearance of hydroxyl bond[24,25].

SEM: SEM images of the synthesized nanocomposites showed (Fig. 4) that all the nano particles were uniformly distributed in the nanocomposite[15]. The results indicate that the particle size increases by addition of aluminum and iron. The addition of aluminum and iron modified the texture of TiO_2/ZnO nanocomposite and affects the average size of particles. It is important for photocatalytic activity that the particle size of the photocatalyst would be homogeneous[9,10,13]. As can be seen,

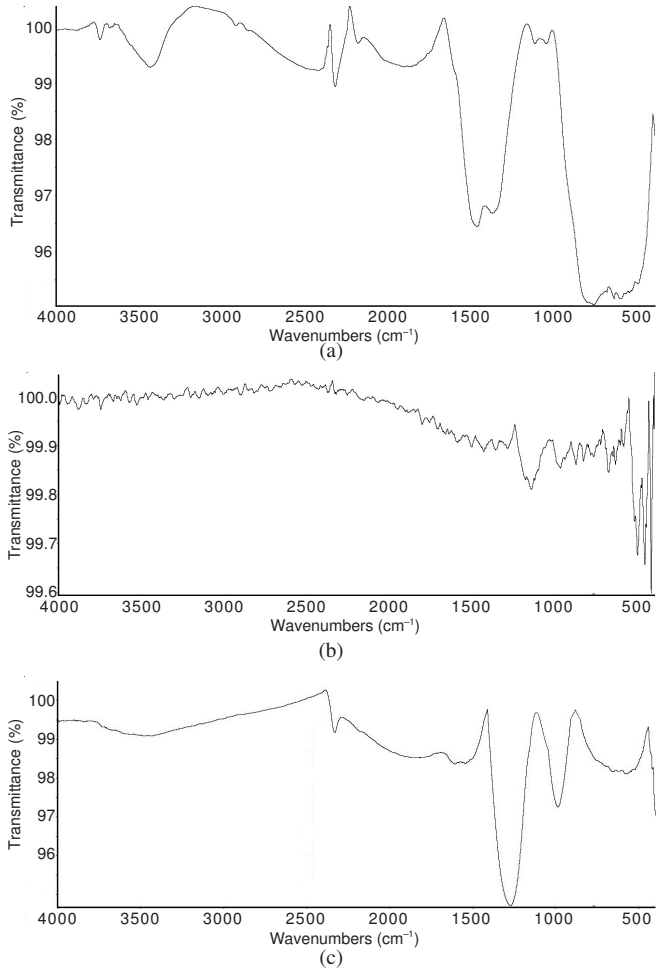

Fig. 3. FT-IR spectra. (a) TiO_2/ZnO, (b) Al- TiO_2/ZnO, (c) Fe-TiO_2/ZnO

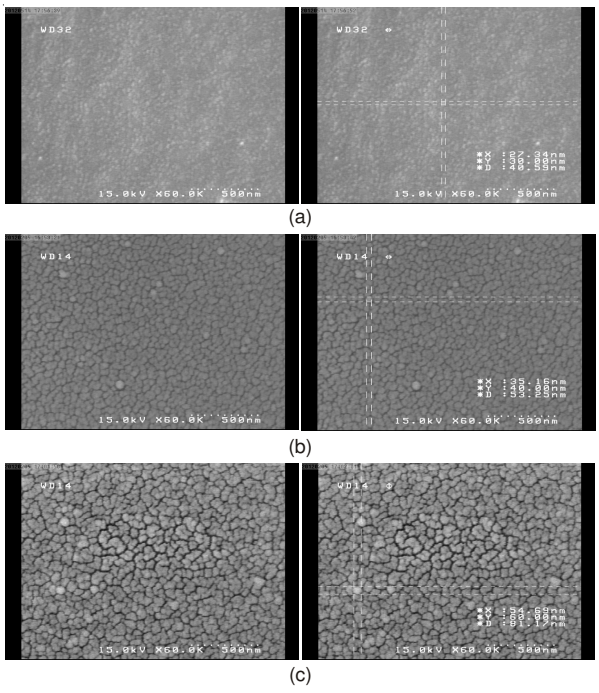

Fig. 4. SEM images analysis of powder samples (a) TiO_2/ZnO, (b) Al-TiO_2/ZnO, (c) Fe-TiO_2/ZnO

SEM images of all sample showed a regular surface without any agglomeration.

XRD: The XRD patterns of samples were shown in Fig. 5. Three remarkable peaks were observed in all samples at 2θ = (25), (27) and (31, 36) which related to anatase, rutile and zincite, respectively[26,27]. As can be seen, anatase phase as the dominant phase has observed in all samples. In Fig. 5a, three phases including, anatase, rutile and zincite were exhibited. In TiO_2/ZnO sample, TiO_2 and ZnO were not doped, however separate crystallization of them was observed. In Fig. 5b, additional phases such as aluminum oxide, aluminum titanium and aluminum titanium oxide phases are composed and they can be seen in 2θ = (52, 67), (26) and (38)[23]. The results showed that aluminum entered into the crystal lattice of titanium dioxide. In Fig. 5c, additional phases (iron titanium and iron titanium oxide phases) are composed and can be seen in 2θ = (42) and (32, 36)[28,29]. The results indicated that iron and aluminum entered into the crystal lattice of titanium dioxide. The crystallite size of samples 1 to 3 is estimated to be 37, 54 and 79 nm, respectively, by using the sherrer equation

$$d = \frac{k\lambda}{\beta \cos\theta}$$

where β (radians) is the full-width of half maximum at 2θ 25.3, k is a constant (0.89), λ is the X-ray wavelength (0.1541 nm for CuK_α), d is the paticle diameter and θ is the angle of

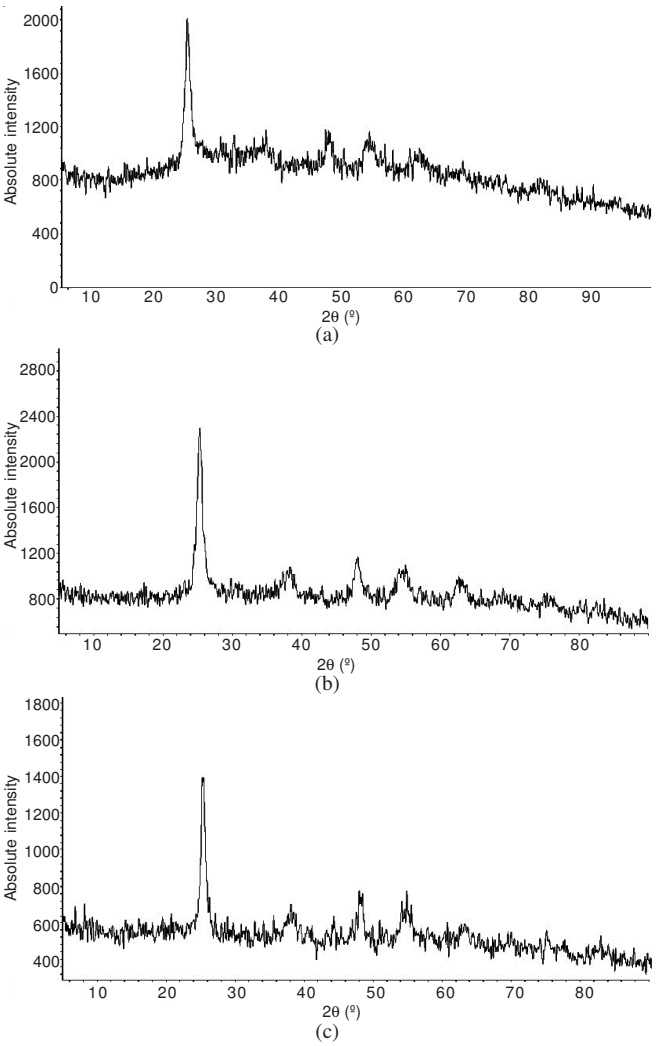

Fig. 5. XRD patterns. (a) TiO_2/ZnO, (b) Al- TiO_2/ZnO, .(c) Fe-TiO_2/ZnO

the diffraction peak (degrees)[30]. The data revealed that addition of aluminum and iron to TiO_2/ZnO affected the particle size of nanocomposite and they increased from 37-79 nm.

Photocatalytic activity: Fig. 6 presents the photocatalytic activity of the synthesized nanocomposites for decolorization of methyl orange in water under UV irradiation in a batch reactor. Complete dye decolorization by TiO_2/ZnO, Al-TiO_2/ZnO and Fe-TiO_2/ZnO were done after 7, 6 and 8.5 h, respectively. With irradiation time elapse of 6 h, the maximum absorbance in visible region of UV-VIS spectra decreased rapidly, which indicates that chromophore of dye is the most active sites for oxidation attack. The results show that the photocatalytic activity increases by adding aluminum and it decreases by adding iron. The photocatalytic activity of Al-TiO_2/ZnO is the best in comparison of other samples.

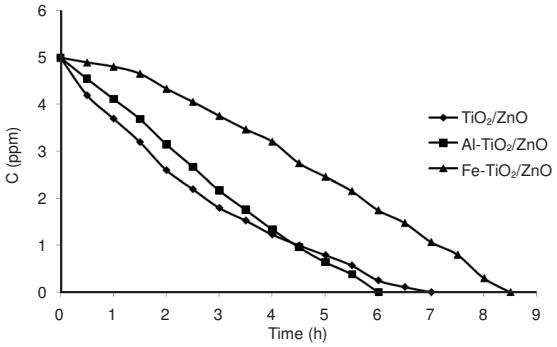

Fig. 6. Decolorization of methyl orange solution under UV radiation using the synthesized composites

Fig. 7 presents the photocatalytic activity of the synthesized nanocomposites for decolorization of methylene blue in water under UV irradiation in a batch reactor. Complete dye decolorization by TiO_2/ZnO, Al-TiO_2/ZnO and Fe-TiO_2/ZnO were done after 4.0, 2.5 and 2.0 h, respectively. With irradiation time elapse of 2 h, the maximum absorbance in visible region of UV-visible spectra decreased rapidly, which indicates that chromophore of dye is the most active sites for oxidation attack. The results show that the photocatalytic activity increases by adding aluminum and Iron and it is superlative in Fe-TiO_2/ZnO nanocomposite. The photocatalytic activity of Fe-TiO_2/ZnO is the best in comparison of other samples. The results showed that the photocatalytic activity of the synthesized nanocomposites for decolorization of methylene blue is more successful than methyl orange.

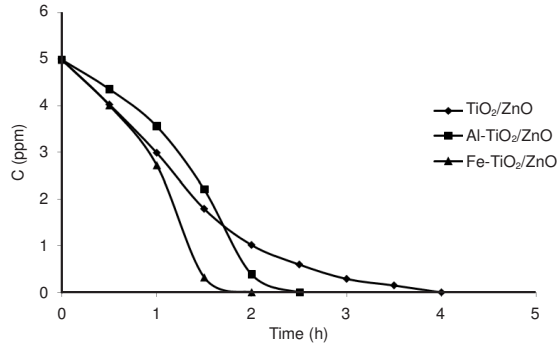

Fig. 7. Decolorization of methylene blue solution under UV radiation using the synthesized composites

Conclusion

The TiO_2/ZnO, Al-TiO_2/ZnO and Fe-TiO_2/ZnO nanocomposites were prepared by sol-gel method. The SEM images indicated that particle size increased by addition of aluminum and iron. It is important for photocatalytic activity that the particle size of the photocatalyst would be homogeneous. The XRD study exhibited that by adding aluminum and iron, the particle size increased from 37-79 nm. The results showed that the photocatalytic activity of the synthesized nanocomposites for decolorization of methylene blue is more successful than methyl orange.

REFERENCES

1. S. Mozia, M. Toyoda, M. Inagaki, B. Tryba and A.W. Morawski, *J. Hazard. Mater*., **140**, 369 (2007).
2. Y. Jiang, Y. Sun, H. Liu, F. Zhu and H. Yin, *Dyes Pigments*, **78**, 77 (2008).
3. C. Chen, Z. Wang, S. Ruan, B. Zou, M. Zhao and F. Wu, *Dyes Pigments*, **77**, 204 (2008).
4. Z. Yuan, J. Jia and L. Zhang, *Mater. Chem. Phys*., **73**, 323 (2002).
5. B. Pal, M. Sharon and G. Nogami, *Mater. Chem. Phys*., **59**, 254 (1999).
6. G. Torres-Delgado, C.I. Zúñiga-Romero, S.A. Mayén-Hernández, R. Castanedo-Pérez and O. Zelaya-Angel, *Sol. Energ. Mater. Sol. C*, **93**, 55 (2009).
7. B. Tryba, *J. Hazard. Mater*., **151**, 623 (2008).
8. H. Yu, X.J. Li, S.J. Zheng and W. Xu, *Mater. Chem. Phys*., **97**, 59 (2006).
9. A. Abdel Aal, M.A. Barakat and R.M. Mohamed, *Appl. Surf. Sci*., **254**, 4577 (2008).
10. D.L. Liao, C.A. Badour and B.Q. Liao, *J. Photochem. Photobiol. A*, **194**, 11 (2008).
11. J. Wang, J. Li, Y. Xie, C. Li, G. Han, L. Zhang, R. Xu and X. Zhang, *J. Environ. Manage*., **91**, 677 (2010).
12. C. Wang, B.Q. Xu, X. Wang and J. Zhao, *J. Solid State Chem*., **178**, 3500 (2005).
13. J. Tian, L. Chen, J. Dai, X. Wang, Y. Yin and P. Wu, *Ceram Int*., **35**, 2261 (2009).
14. R. Pérez-Hernández, D. Mendoza-Anaya, M.E. Fernández and A. Gómez-Cortés, *J. Mol. Catal. A*, **281**, 200 (2008).
15. J. Tian, L. Chen, Y. Yin, X. Wang, J. Dai, Z. Zhu, X. Liu and P. Wu, *Surf. Coat. Technol*., **204**, 205 (2009).
16. K. Karthik, S.K. Pandian and N.V. Jaya, *Appl. Surf. Sci*., **256**, 6829 (2010).
17. M.H. Liao, C.H. Hsu and D.H. Chen, *J. Solid State Chem*., **179**, 2020 (2006).
18. B.A. Sava, A. Diaconu, M. Elisa, C.E.A. Grigorescu, C. Vasiliu and A. Manea, *Superlattices Microst*., **42**, 314 (2007).
19. X.T. Wang, S.H. Zhong and X.F. Xiao, *J. Mol. Catal. A*, **229**, 87 (2005).
20. L. Chen, B.Y. He, S. He, T.J. Wang, C.L. Su and Y. Jin, *Powder Technol*., **227**, 3 (2012).
21. A. Glisenti, *J. Mol. Catal. A*, **153**, 169 (2000).
22. S.D. Lin, A.C. Gluhoi and B.E. Nieuwenhuys, *Catal. Today*, **90**, 3 (2004).
23. I.H. Joe, A.K. Vasudevan, G. Aruldhas, A.D. Damodaran and K.G.K. Warrier, *J. Solid State Chem*., **131**, 181 (1997).
24. B. Khodadadi, M. Sabeti, S. Moradi, P. Aberomand Azar and S.R. Farshid, *J. Appl. Chem. Res*., **20**, 36 (2012).
25. P. Aberomand-Azar, S. Moradi-Dehaghi, S. Samadi, S. Kamyar and M. Saber-Tehrani, *Asian J. Chem*., **22**, 1619 (2010).
26. K. Oyoshi, N. Sumi, I. Umezu, R. Souda, A. Yamazaki, H. Haneda and T. Mitsuhashi, *Nucl. Instrum. Meth. B*, **168**, 221 (2000).
27. M.R. Vaezi, *J. Mater. Process Technol*., **205**, 332 (2008).
28. F. Zhou, S. Kotru amd R.K. Pandey, *Thin Solid Films*, **408**, 33 (2002).
29. R. Shi, C. Bai, M. Hu, X, Liu and J. Du, *J. Min. Metall. Sect B-Metall*., **47**, 99 (2011).
30. C.C. Chan, C.C. Chang, W.C. Hsu, S.K. Wang and J. Lin, *Chem. Eng. J*., **152**, 492 (2009).